Physics Letters B 752 (2016) 212–216

Contents lists available at ScienceDirect

Physics Letters B

www.elsevier.com/locate/physletb

Improved measurement of the neutron absorption cross section for very low velocities

J. Schroffenegger [a,d,*], P. Fierlinger [b], A. Hollering [d], P. Geltenbort [c], T. Lauer [d], H. Rauch [a], T. Zechlau [d]

[a] Technische Universität Wien-Atominstitut, A-1020 Wien, Austria
[b] Physik-Department E18, Technische Universität München, D-85748 Garching, Germany
[c] Institut Laue-Langevin, F-38042 Grenoble, France
[d] Forschungs-Neutronenquelle Heinz Maier-Leibnitz (FRM-II), 85747 Garching, Germany

ARTICLE INFO

Article history:
Received 2 March 2015
Received in revised form 26 October 2015
Accepted 11 November 2015
Available online 14 November 2015
Editor: D.F. Geesaman

Keywords:
Neutron transport: diffusion and moderation
Protons and neutrons

ABSTRACT

The absorption cross section of natural Gd and isotopic enriched ^{157}Gd for ultra-cold neutrons (UCN) as a function of the velocity has been measured within a time-of-flight-experiment. Particular attention is paid to small velocities in the region of a few m/s. This is intended to determine the validity of the $1/v$-law governing absorption cross sections in this region and the resulting divergence at $v = 0$. The experiment does not show any significant violation of $1/v$ for $v > 3$ m/s.

1. Introduction

The neutron absorption cross section can be described, leaving aside resonance phenomena, in the first order approximation by a $1/k$ or $1/v$ law [1]:

$$\sigma_a = \frac{4\pi}{k} a'', \tag{1}$$

where a'' is the imaginary part of the scattering length, v is the neutron velocity and k is the neutron wave-vector. This equation raises the question of the divergent tendency of the absorption cross section at low velocities close to $v = 0$ and of its physical meaning. In [2] a deviation of the $1/v$ law is predicted. The authors arrived at this result by theoretical calculation of the interaction between an absorbing nucleus and a neutron. It is expected that the cross section is proportional to v in the region below 4–5 m/s. The authors of [3] however, conclude that the result found in [2] concerns only the effective cross section for a nucleus occurring in a dense medium and not for a single nucleus or for an absorber dissolved in a solvent at low concentration. The present work incorporates these conclusions. In [4] the authors show the validity of the $1/v$-law for velocities between 6 and 35 m/s by verifying the independence of the transmission through an absorbing film from the neutron velocity component parallel to the sample surface.

Another way for testing the $1/v$-law is examined in [5] by using a time-of-flight-setup. Using this method the absorption cross section for all velocities contained in the spectrum of the neutron source can be measured simultaneously. The authors show in their results a possible violation of the $1/v$ law. The measurements described in the present work can be considered as a continuation of the experiments performed in [5].

2. Experimental approach

In this experiment gadolinium, the stable element with the highest neutron absorption cross section[1] dissolved in heavy water (D_2O), is used as an absorber. This enables the smallest amount of absorbent material to be brought into solution whilst maintaining ideal proportions for the transmission coefficient. The low concentration of the absorber in the D_2O-matrix does not noticeable change the real part of the scattering length density in the

* Corresponding author at: Forschungs-Neutronenquelle Heinz Maier-Leibnitz (FRM-II), 85747 Garching, Germany.
E-mail address: juri.schroffenegger@tum.de (J. Schroffenegger).

[1] Thermal neutron absorption cross sections: nat. Gd $\sigma_a = 49700$ barn, isotipcal enriched ^{157}Gd $\sigma_a = 259\,000$ barn.

http://dx.doi.org/10.1016/j.physletb.2015.11.030

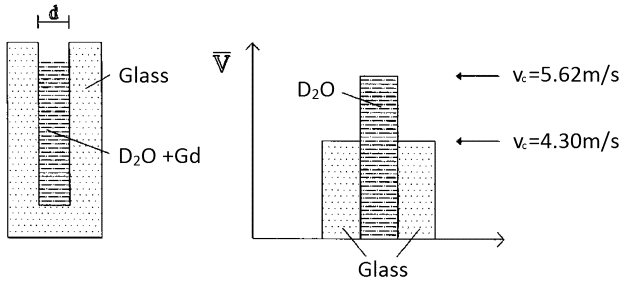

Fig. 1. Geometrical form and neutron optical wall potential of the transmission samples.

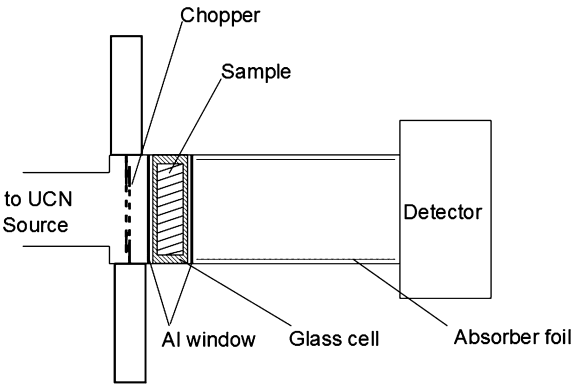

Fig. 2. Sketch of the time of flight setup on the UCN beam port on the PF2 beamline at ILL.

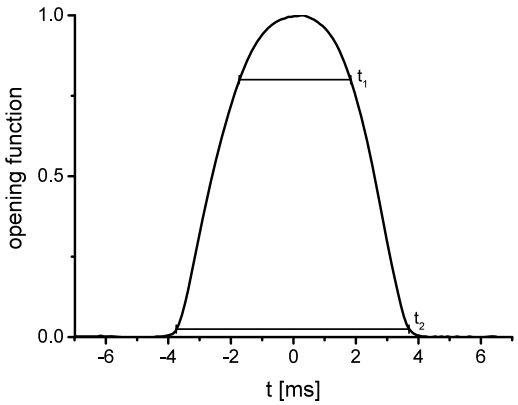

Fig. 3. Measured opening function of the linear chopper with $t_1 = 3.44(14)$ ms: duration of the opening larger than 90%, $t_2 = 7.47(7)$ ms: duration of the opening larger than 2.5%.

transmission sample. The advantage of the method is its large scattering length and the resulting high Fermi-potential. As they enter the potential of the D_2O neutrons lose a part of their kinetic energy and decelerate. The velocity inside the sample is given by

$$v = nv_0 = \sqrt{{v_0}^2 - {v_c}^2} \text{ with } {v_c}^2 = \frac{4\pi\hbar^2 N b_c}{m^2} \tag{2}$$

where n is the refraction index, v_0 is the velocity outside the potential, N is the particle density, b_c is coherent scattering length and m is the mass of the neutron. By decelerating the neutrons in the sample it is possible to achieve lower velocities, than those present in the neutron source's spectrum. The liquid solution is brought into the neutron beam within a glass cell. In Fig. 1 the potential for a neutron crossing the sample is shown. To determine the absorption cross section of the gadolinium, a second identical sample without dissolved gadolinium is used. By comparing the transmission through both samples the absorption cross section σ_a can be calculated as:

$$T = e^{-Nd\sigma_a} \rightarrow \sigma_a = -\ln\frac{T}{Nd} \tag{3}$$

with T the transmission, N the particle density and d the thickness of the absorber. To calculate the transmission and the related absorptions cross section as a function of the velocity, the sample is installed within a time-of-flight setup. The ratio of the count rate for the samples with gadolinium to the count rate without gadolinium provides the absorption cross section.

3. Experimental setup

The time-of-flight-measurements (TOF) described were performed at ultra-cold and very-cold neutron facility PF2 of the ILL in Grenoble (France). Two different beam ports were used: Pf2/UCN and PF2/TES.

In order to soften the spectrum and thus shift the neutron velocity spectrum to lower energies, the TOF setup presented in Fig. 2 was mounted 60 cm higher than the existing turbine exit of the PF2/UCN port. At the PF2/TES port, however, it was mounted at the same height as the exit port. An UCN chopper [6] composed of two linear motors moving two titanium grids against each other forms the first element of the TOF setup. The grids in their starting position overlap 1 mm. In this position the beam is closed, so that no neutron can pass through. Shifting the grids by 2 mm opens a 3 mm slit and enables the neutrons to pass. A chopper of this type provides variable opening times and duty cycles, in contrast to a rotating disk chopper. This allows the open-to-close ratio to be optimized and thus increases the number of the usable neutrons. The chopper is set to open the beam for 7 ms with a repetition rate of 10 Hz. The corresponding opening function, measured with light, is shown in Fig. 3. The chopper setup is a well characterized system; the variation of the open function is less than 1%. A cell holder for the heavy water samples integrated into the stainless steel chopper housing is positioned almost at the beginning of the flight path. The chopper vacuum, the UCN feed guide and the flight path are separated from the glass cell by two 0.2 mm thick foils of $AlMg_3$. By keeping the sample at atmospherical pressure it can be changed easily without breaking vacuum.

The glass cell itself is composed of three layers of sodium-glass glued together with ultraviolet curing glue. A cavity in the center layer forms the filling volume of the cell. The internal dimensions of the cell are $60 \times 90 \times 1.02$ mm^3. The thickness of the outer glass plates is 0.9 mm. The flight path, a stainless steel tube with a diameter of 100 mm and an effective flight path length of 263.5 mm is installed on the backside of the cell holder. A polyethylene foil, placed on the inside of the tube acts as an absorber, removing neutrons which would otherwise be reflected by the tube. This ensures that any diffusive scattering, which would falsifying the TOF spectrum, is suppressed. This effect was investigated in a separate measurement, performed with and without the polyethylene foil. The spectra of the neutron passing through the cell filled with D_2O were observed. The results shown in Fig. 4, obtained without the PE foil, show a relatively increased number of neutron at the slow velocity side of the spectrum, caused by diffuse scattering. The flight path follows a CASCADE U-100 [8] detector.

The transmission experiment was performed with four different gadolinium solutions, varying in particle density and the isotopic distribution. The four Gd solutions measured were natural gadolinium with a particle density of $6.66 \cdot 10^{23}$ 1/m^3 and of $4.04 \cdot 10^{23}$ 1/m^3 and isotopic pure ^{157}Gd with a particle density

Table 1
Measured absorption cross section of the four different gadolinium solutions with Poison type error $\Delta\sigma_P$ and Gaussian type $\Delta\sigma_G$.

	N	Beamport	σ [Mb]	$\Delta\sigma_P$ [Mb]	$\Delta\sigma_P/\sigma$ [%]	$\Delta\sigma_G$ [Mb]	$\Delta\sigma_G/\sigma$ [%]
3 m/s							
nat. Gd	6.66	UCN	17.28	2.91	16.9	3.3	19.1
nat. Gd	4.04	UCN	29.5	7.33	15.8	5.81	19.7
^{157}Gd	1.40	UCN	96.70	18.85	19.5	21.98	22.7
^{157}Gd	1.39	TST	102.54	20.27	19.8	2.82	2.7
5 m/s							
nat. Gd	6.66	UCN	11.33	0.24	2.1	3.30	29.1
nat. Gd	4.04	UCN	18.85	0.54	2.9	5.82	30.9
^{157}Gd	1.40	UCN	77.87	1.50	1.9	21.98	28.2
^{157}Gd	1.39	TST	73.17	1.60	2.2	2.82	3.8
10 m/s							
nat. Gd	6.66	UCN	5.36	0.09	1.74	3.30	61.6
nat. Gd	4.04	UCN	10.58	0.21	2.0	5.82	55
^{157}Gd	1.40	UCN	47.69	0.52	1.1	21.98	46.1
^{157}Gd	1.39	TST	40.64	0.49	1.2	2.82	6.9

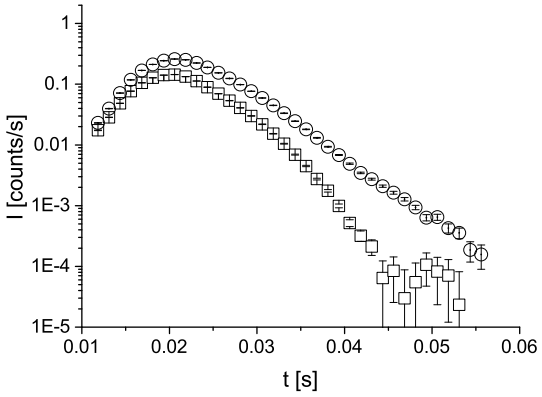

Fig. 4. Time-of-flight (TOF) spectra measured for pure D_2O with polyethylene foil ○ in the flight path and without □.

of $1.4 \cdot 10^{23}$ 1/m^3 and $1.39 \cdot 10^{23}$ 1/m^3. An acidic environment is required to dissolve gadolinium in heavy water. For this reason a small amount (<200 ppm) of DCl was added to the D_2O. As in all the other measurements taken with Gd solutions of this sort, contamination by DCl was found to be insignificant for further data analysis. The reference measurement was performed with pure (99.98%) D_2O from the same batch as used for the Gd solution.

4. Experimental results and their analysis

The time-of-flight-spectra time resolution is given by the brought of the detector time channels, which was set to 250 μs. A single spectrum was measured for 130 s, what was repeated up to 1500 times. The small peak shortly after the start, i.e. 0 s, is caused by UCN up-scattered in cells glass and in the heavy water. After subtracting a constant background (caused by the thermal neutron background in the reactor environment), the velocity-dependent transmission is obtained by comparing the counts for a single time bin for measurements with the gadolinium solution and pure D_2O. Finally, the absorption cross section can be extracted as a function of the neutron velocity, presented in Fig. 5, by applying three important corrections:

- the position of the sample behind the chopper. The time of flight is changed because the neutrons are decelerated in the potential of the sample. Fig. 6 shows the correlation of the time neutrons need to cross the flight path with and without sample inserted.
- neutrons, reflected at the D_2O surface, leading to multiple crossing of the sample [7]. Considering this effect, the transmission coefficient is given as

$$\tau = \frac{\alpha T^2}{1 - \alpha^2 R^2} \tag{4}$$

with $\alpha = e^{-N\sigma d}$, $T = \frac{4v_0 Re(v')}{|v_0+v'|^2}$ and $R = |\frac{v_0-v'}{v_0+v'}|^2$ where T is the transmissivity and R is the reflectivity of the D_2O surface. Both values depend on the UCN velocity outside the sample, v_0 and on the, in general complex, velocity v' inside the sample. σ is the sum of the inelastic and incoherent scattering cross section, which is dominated by the absorption. Without multiple crossings the transmission coefficient would reduce to α as expected.
- the UCN velocity within the potential of the D_2O, calculated according eqn. (2).

The results of the measurements performed at the UCN beam provide no absolute value for the absorption cross section within acceptable error limits, because the total count rate for the single 130 s spectra is fluctuating, as shown in Fig. 7. This fluctuation produces an additional Gaussian type error for the calculation of the absolute value. In Table 1 absolute values and error limits for the different performed measurements are listed. Hereby the error limits are distinguished in the mentioned Gaussian error and the error given by Poison statistics, which depends on the total counts of a single measurement. The results of the two measurements, performed on different beams, match and yield Poisson-type errors in the same region. But in contrast to the TST beam measurement, the UCN beam measurement shows very large Gaussian type errors, with relative errors up to 46.1%. Nevertheless the dependence of the absorption cross section on the velocity can be calculated. The results shown in Fig. 5 a)–c) do not include the additional error caused by the fluctuation. The measurement performed at the TST beam port does not show a significant fluctuation of the count-rate. For that reason the absolute value of the cross section can be calculated and are within acceptable error limits, shown in Fig. 5 d).

To evaluate the behavior of the absorption cross section the measured data can be fitted with different functions, like $1/v$, becoming constant or proportional to v at a certain velocity. The different models can be compared using the reduced χ^2 values and the corresponding p values. In Table 2 the such values are listed for the fit models mentioned.

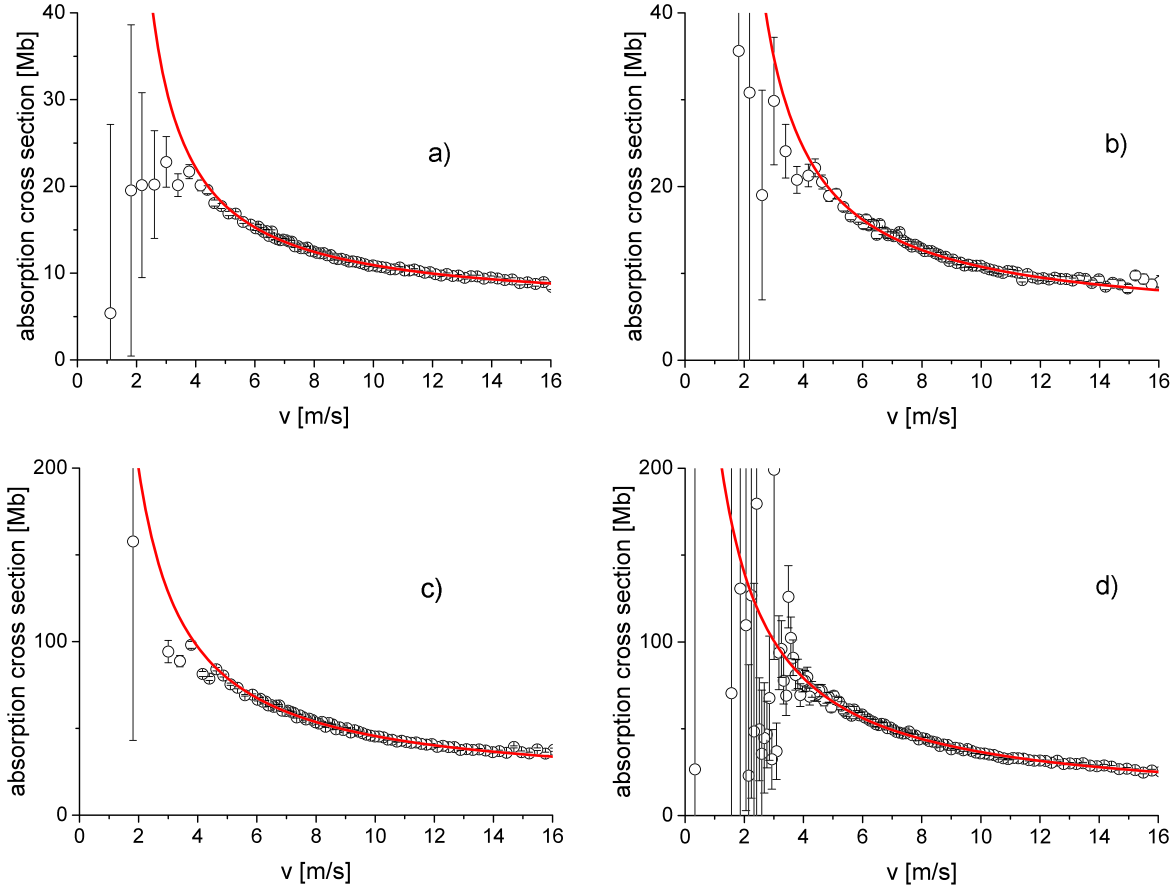

Fig. 5. Extracted absorption cross section as function of the velocity; line: $1/v$-law, a) Gd(nat) $6.66 \cdot 10^{23}$ $1/m^3$, b) Gd(nat) $4.04 \cdot 10^{23}$ $1/m^3$, c) ^{157}Gd $1.40 \cdot 10^{23}$ $1/m^3$, d) ^{157}Gd $1.39 \cdot 10^{23}$ $1/m^3$.

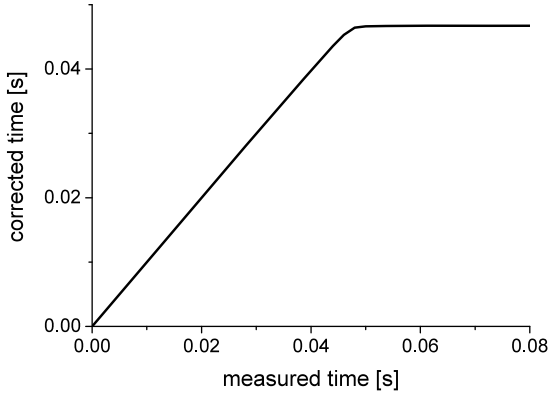

Fig. 6. Correlation of the measured time of flight and the theoretical without sample.

Table 2
Reduced χ^2 and p values (117 degrees of freedom) for different fitting models. 4.46 m/s and 3.66 m/s are the optimized velocities for the corresponding fitting model.

Fitting function	v_0 [m/s]	χ^2	p value
$\sigma_a \propto \frac{1}{v}$		1.78	$1.3 \cdot 10^{-6}$
$\sigma_a \propto \frac{1}{v}$, $v > v_0$	5	1.57	$1.9 \cdot 10^{-4}$
$\sigma_a \propto$ const, $v < v_0$	4	1.37	$9.5 \cdot 10^{-3}$
	3	1.67	$2.2 \cdot 10^{-5}$
	4.46	1.35	$1.5 \cdot 10^{-2}$
$\sigma_a \propto \frac{1}{v}$, $v > v_0$	5	3.6	$2.4 \cdot 10^{-24}$
$\sigma_a \propto v$, $v < v_0$	4	1.32	$2.0 \cdot 10^{-2}$
	3	1.58	$1.5 \cdot 10^{-4}$
	3.66	1.27	$4.8 \cdot 10^{-2}$

5. Conclusion

In the measurement described, we measured the neutron absorption cross section for Gd. The results show values, depending on velocity, up to 100 Mb. The $1/v$-law was also examined. Contrary to [5], no significant violation in the region above 3 m/s was visible. One possible explanation for this is the improved experimental setup, and the polyethylene absorber foil in particular. This foil eliminates non-angular reflected neutrons. The pollution of the spectrum due to these neutrons is shown in Fig. 8 for a flight path of 263.5 mm. A longer flight path, as used in the previous experiments, influences the results even more strongly. More specifically it leads to an overrating of the neutron transmission on the lower flanks of the spectrum.

By fitting models to the data measured, we obtained slightly better reduced χ^2 values than those obtained with the $1/v$-law; this was not sufficient, however, to demonstrate any significant violation of the $1/v$-law. The lack of data in the velocity region below 3 m/s inhibits any further extrapolation of the absorption cross section. Further investigations would be needed to obtain more precise results at even lower velocities. Nevertheless the possibilities of this approach are rather limited and significant improvements on the error limits in the lower velocity range are not

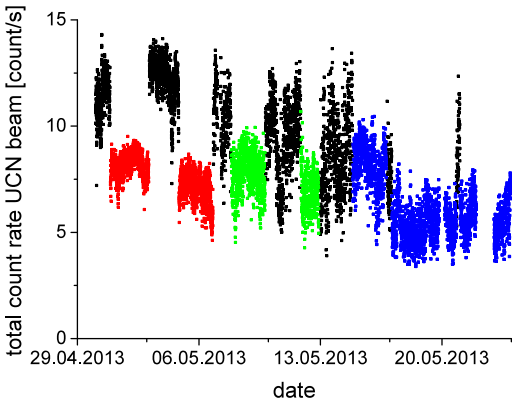

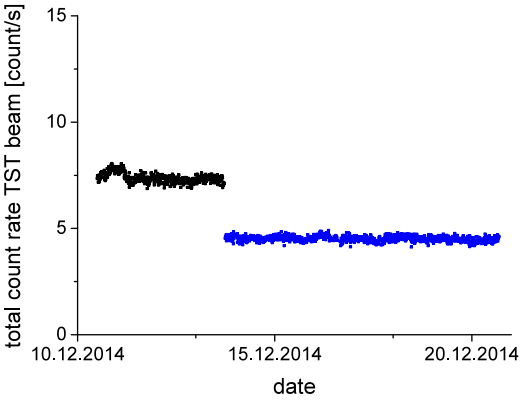

Fig. 7. Total count rate for UCN beam and TST beam experiments. UCN beam: black: pure D_2O fluctuation for the full spectrum 20%, red: Gd(nat) $6.66 \cdot 10^{23} 1/m^3$ fluctuation 10.3%, green: Gd(nat) $4.04 \cdot 10^{23}$ $1/m^3$ fluctuation 13.3%, blue ^{157}Gd, $1.40 \cdot 10^{23}$ $1/m^3$ fluctuation 24.4% TST beam: black: pure D_2O fluctuation 3%, blue ^{157}Gd, $1.39 \cdot 10^{23}$ $1/m^3$ fluctuation 2.6%.

to be expected. Another approach will be necessary for future investigations.

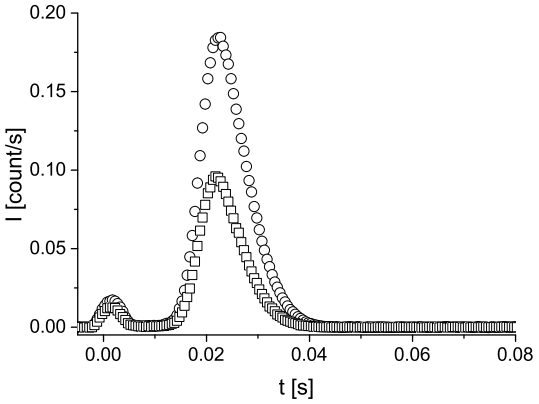

Fig. 8. Time-of-flight (TOF) spectra measured for pure D_2O ◯ and Gd-solution □ normalized to their total measurement time.

Acknowledgements

This experiment benefited from the technical support by T. Brenner and D. Hess from the ILL and J. Weber form the neutron optic group of the FRM II. The kind hospitality of the ILL is gratefully acknowledged. This work was supported by the DFG under the contract number La 2835/1-1.

References

[1] V.F. Sears, Neutron Optics, Oxford University Press, 1989.
[2] V.V. Lomonosov, A.I. Gurevich, Capture of ultracold neutrons in thin absorbing films, J. Exp. Theor. Phys. 95 (5) (2002) 800–804.
[3] A.I. Frank, V.I. Bodnarchuk, P. Geltenbort, et al., Phys. At. Nucl. 66 (10) (2003) 1831–1845.
[4] A.I. Frank, P. Geltenbort, G.V. Kulin, et al., JETP Lett. 3 (2006) 105–109.
[5] H. Rauch, M. Zawisky, C. Stellmach, P. Geltenbort, Phys. Rev. Lett. 83 (24) (1999) 4955–4958.
[6] T. Lauer, Investigation of a superthermal ultracold neutron source based on a solid deuterium converter for the TRIGA Mainz reactor, Dissertation, 2010.
[7] A. Steyerl, Nucl. Instrum. Methods 101 (1972) 295–314.
[8] http://www.n-cdt.com.